



**SEARCH FOR Ξ^{*-} , Σ^{*-} , AND Ω^{-} PRODUCTION
BY NEGATIVE HYPERONS ON NUCLEI**

V. Hungerbühler, R. Majka, J. N. Marx, P. Némethy,
J. Sandweiss, W. Tanenbaum, and W. J. Willis
Yale University, New Haven, Connecticut 06520 USA

and

M. Atac, S. Ecklund, P. J. Gollon, J. Lach, J. MacLachlan,
A. Roberts, R. Stefanski, and D. Theriot
National Accelerator Laboratory, Batavia, Illinois 60510 USA

and

C. L. Wang
Brookhaven National Laboratory, Upton, New York 11973 USA

and

W. Cleland, E. Engels, Jr., D. I. Lowenstein,
N. Scribner, and J. Thompson
University of Pittsburgh, Pittsburgh, Pennsylvania 15260 USA

March 1974



SEARCH FOR Ξ^{*-} , Σ^{*-} , AND Ω^{-} PRODUCTION
BY NEGATIVE HYPERONS ON NUCLEI

V. Hungerbühler, * R. Majka, J. N. Marx, P. Némethy,
J. Sandweiss, W. Tanenbaum, and W. J. Willis[†]
Yale University, New Haven, Connecticut 06520 USA[‡]

and

M. Atac, S. Ecklund, P. J. Gollon, J. Lach, J. MacLachlan,
A. Roberts, R. Stefanski, and D. Theriot
National Accelerator Laboratory, Batavia, Illinois 60510 USA

and

C. L. Wang
Brookhaven National Laboratory, Upton, New York 11973 USA^{||}

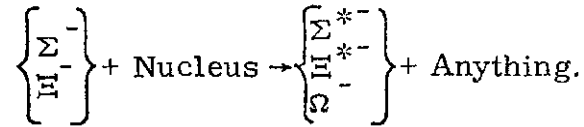
and

W. Cleland, E. Engels, Jr., D. I. Lowenstein,^{**}
N. Scribner,^{††} and J. Thompson
University of Pittsburgh, Pittsburgh, Pennsylvania 15260 USA^{‡‡}

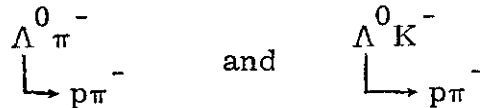
ABSTRACT

The reactions of 24.6 GeV/c Σ^{-} and Ξ^{-} incident on a scintillator target were studied in a counter-spark chamber experiment. Upper limits on the production cross section of Σ^{*-} resonances which decay into $\Lambda^0 \pi^{-}$, and of Ξ^{*-} resonances which decay into $\Lambda^0 K^{-}$ were obtained. A single Ω^{-} that was produced in the scintillator target has been observed, corresponding to a 115 $\mu\text{b}/\text{nucleon}$ production cross section if produced by a Ξ^{-} . The $\Lambda^0 \pi^{-}$ mass spectrum was found to be consistent with a Deck-type threshold enhancement.

We report the results of a search for hyperon resonance and Ω^- production by negative hyperons incident on a plastic scintillator target:



The experiment was performed in the high-energy negative hyperon beam at the Alternating Gradient Synchrotron (AGS) of the Brookhaven National Laboratory. Scintillator and spark-chamber arrays were used to identify the final states



from resonance or Ω^- decay, and to measure their effective mass.

The hyperon beam is a short, curved magnetic channel that delivers fluxes of approximately $200 \Sigma^-$ and $2 \Xi^-$ per 1.5×10^{11} interacting protons, at a momentum of $24.6 \text{ GeV}/c$. Figure 1 is a plan view of the hyperon beam and detection apparatus, which is described in detail elsewhere.¹ Beam particles of mass less than $1 \text{ GeV}/c$ ² are tagged and vetoed by a threshold Cerenkov counter (C_B) which forms part of the magnetic channel. A high-pressure, high-resolution ($\sigma < 100 \mu\text{m}$) magnetostrictive spark chamber² measures the momentum (to $\pm 1\%$) and direction (to $\pm 0.5 \text{ mrad}$) of hyperons emerging from the channel. Small scintillation counters (B) define the beam. A hole veto counter (V_H) downstream of the high resolution spark chambers discriminates against beam halo and upstream hyperon decays.

A 5 cm × 5 cm × 25 cm long plastic scintillator production target follows the high resolution spark chambers. The pulse height from this target is recorded for each event to help differentiate between diffractive and nondiffractive production processes. Downstream of the target a scintillator-lead-scintillator sandwich, with a hole for forward interaction products, serves to tag gamma rays from the target.

Located downstream from the 1.5 m long decay region is a double magnetic spectrometer with conventional magnetostrictive spark chambers. The first spectrometer analyzes the relatively low momentum (< 10 GeV/c) π^- and K^- mesons from the target or from hyperon decays. The second spectrometer measures the momentum of the high-energy protons from $\Lambda^0 \rightarrow p\pi^-$ decays. The field integrals of the two magnets are 13 kG-m and 26 kG-m respectively, so that particle momenta are typically determined to between 2 and 5%. A counter hodoscope (S) between the spectrometer magnets serves to trigger on one or more slow negative particles. Two proton counters (P) and an iron-scintillator calorimeter (PC) define a proton trigger. The calorimeter rejects background muons which can otherwise simulate good triggers. A large phase space threshold Cerenkov counter between the two spectrometer magnets separates $\Lambda^0\pi^-$ from Λ^0K^- final states. This counter, which is filled with N_2O at atmospheric pressure,³ is sensitive to pions and kaons with momenta above 4.8 GeV/c and 16.8 GeV/c respectively, and is therefore used to separate π^- from K^- in the momentum range of 5 to 12 GeV/c.

The trigger for either final state coming from the interaction of an incident hyperon is

$$\overline{C}_B \cdot B \cdot \overline{V}_H \cdot S \cdot P \cdot PC.$$

This signals a massive beam particle, a fast proton and one or more relatively slow negative particles. The trigger rate was a few per AGS pulse. For each event we recorded the configuration of scintillation counter hits, data from the spark-chamber readouts, and pulse heights from the target scintillator, the Cerenkov counters, calorimeter, and γ counters.

To be accepted for analysis, events were required to have a topology consistent with one positive and two negative tracks. In addition, the following criteria were required of the events: a beam track consistent with a trajectory from the hyperon production target through the magnetic channel; all tracks within a restricted fiducial volume; a minimum angle of 10 mrad between the Λ^0 and the negative particle in the $\Lambda^0 \pi^-$ (or $\Lambda^0 K^-$) decay; a distance of closest approach of less than 0.5 cm at the production vertex and 0.4 cm at the Λ^0 decay vertex; and a Λ^0 decay length which is greater than zero, allowing for a longitudinal vertex reconstruction error of 20 cm.

The pion from Λ^0 decay was identified by reconstructing the $\pi\pi^-$ effective mass for each negative particle in turn. In Fig. 2 the clean, narrow peak (~ 4 MeV fwhm) in the $\pi\pi^-$ mass spectrum at the Λ^0 mass contains solutions with a correct choice of the negative track, while the

broad spectrum at higher mass contains the incorrect pairings. Any solution for which the $p\pi^-$ invariant mass is within 5 MeV of the Λ^0 mass was chosen. Even if the pairing ambiguity were not correctly resolved, there would be no effect on the invariant mass of $p\pi^-\pi^-$ final states and only a small effect on that of $p\pi^-K^-$ final states.

Figure 3(a) shows the $p\pi^-\pi^-$ invariant mass spectrum for events whose decay vertex lies inside the scintillator target, after the above cuts were made. In addition to production in the target we see a sharp peak at the Ξ^- mass. The trigger is thus seen to be dominated by beam Ξ^- 's. In the analysis, a minimum angle requirement of 5 mrad between the momentum vector of the incident hyperon and that of the outgoing $\Lambda^0\pi^-$ system serves to discriminate against the beam Ξ^- . Figure 3(b) shows the resulting spectrum. We interpret the remaining Ξ^- peak as those beam Ξ^- which elastically scattered in the scintillator target. Events with a vertex downstream of the target show the cascade peak only.

There is no evidence for the Σ^{*-} resonances in the spectrum from the target [Fig. 3(b)]. After subtracting the remnant beam cascades as determined from the number seen decaying in the decay region, a broad enhancement remains at the mass threshold [shaded region in Fig. 3(b)]. A Monte Carlo calculation, starting with the simplest Deck-effect⁴ matrix element [Fig. 4(a)] and simulating the acceptance of our apparatus, gives the predicted invariant mass spectrum shown in Fig. 4(b). The Deck-effect prediction closely resembles the shape of our data

[shaded portion of Fig. 3(b)]. The inclusion of other Deck diagrams would not change this result since the predicted shape of the mass distribution is strongly influenced by our detection efficiency, which is limited by the magnet apertures and decreases rapidly above 1400 MeV, as shown in Fig. 5(a). (The reason for this strong dependence of detection efficiency on resonance mass is that the spectrometers were designed for use in studies of hyperon production⁵ and leptonic decays.⁶) Figure 5(b) shows the upper limit on the cross section for resonance production of Σ^{*-} as a function of the Σ^{*-} mass.

The absence of a signal from the $\Sigma^{*}(1385)$ resonance is an interesting feature of the data. We put an upper limit (90% confidence level) of $80\mu\text{b}$ on the production of this resonance, assuming a width of 40 MeV. Its absence may be due to the fact that the production of the $\Sigma^{*}(1385)$ from a Σ^{-} requires unnatural spin-parity exchange, as well as the exchange of SU_3 quantum numbers.⁷ Either of these factors can prevent $\Sigma^{*}(1385)$ production by Pomeron exchange. Production of $\Sigma^{*}(1385)$ by π exchange is possible, but the cross section for this process is small at the present energies.

One aim of this experiment was to detect the production of the strange SU_3 analogues of the $N^{*}(1470)$. The masses of such states, if they exist, may well be beyond the acceptance of this apparatus. If not, then either the production of, or the two-body decay of these states must be suppressed. The inhibition of such two-body decays is predicted by a quark model of Lipkin.⁸

Candidates for Ξ^{*-} resonances and Ω^- production $\Lambda^0 K^-$ final states were selected by requiring that the meson that is not from the Λ^0 decay be within the geometric acceptance and valid momentum range of the N_2O Cerenkov counter. This counter was then used as a pion veto. There is no evidence of ΛK^- production in the sample of events with vertices in the scintillator target. Figure 6(a) shows the apparatus acceptance as a function of Ξ^{*-} mass, and Fig. 6(b) shows the experimental upper limit on the cross section for the production of a single Ξ^{*-} in our mass region.

Events with a $\Lambda^0 K^-$ vertex in the decay region were analyzed for Ω^- decays since there was no background from target excitations in this region. One possible Ω^- event was found in this data sample. This event, which was produced in the scintillator target, has a reconstructed Λ^0 mass of $1118 \text{ MeV}/c^2$ and a reconstructed $p\pi^- K^-$ mass of $1676 \text{ MeV}/c^2$. A large pulse height was observed in the target scintillator with a large ($7.36 \text{ GeV}/c$) imbalance in longitudinal momentum. These signals are characteristic of a highly inelastic event needed to produce an Ω^- in a $Y^- N$ reaction. However, the high spark multiplicity of this event does not permit its unambiguous interpretation. Using a Monte-Carlo calculation of our acceptance we find that one event would correspond to an Ω^- production cross section of $115 \mu\text{b}/\text{nucleon}$ if it were caused by an incident Ξ^- , and $1 \mu\text{b}/\text{nucleon}$ if caused by a Σ^- . The corresponding 90% confidence limits are $\sigma < 450 \mu\text{b}/\text{nucleon}$ and $\sigma < 5 \mu\text{b}/\text{nucleon}$, respectively.

We wish to thank our engineering staff, Satish Dhawan, Cordon Kerns, and Blaise Lombardi, and our technicians Jon Blomquist, Ed Steigmeyer, Alan Wandersee, and Ralph Berner for their help in the design and setup of the apparatus. We also thank the AGS staff, in particular David Berley, for providing the technical support needed for the success of this experiment.

FOOTNOTES AND REFERENCES

* Present address: Dept. de Physique Nucléaire et Corpusculaire,
Université de Genève, Geneva, Switzerland.

† Present address: CERN, 1211 Geneva 23, Switzerland.

‡ Research supported by the United States Atomic Energy Commission
under Contract AT(11-1).

|| Supported by the United States Atomic Energy Commission.

** Present address: Brookhaven National Laboratory, Upton, New York.

†† Present address: Bell Laboratories, Holmdell, New Jersey 07733.

‡‡ Supported in part by the United States National Science Foundation.

¹ V. Hungerbühler et al. , The Design and Operation of the Yale-NAL-
BNL Hyperon Beam, Nucl. Instr. and Methods, to be published.

² W. J. Willis et al. , Nucl. Instr. and Methods 91, 33 (1971).

³ With an index of refraction of 1.000516.

⁴ R. T. Deck, Phys. Rev. Letters 13, 169 (1964).

⁵ V. Hungerbühler et al. , Phys. Rev. Letters 24, 1234 (1973).

⁶ V. Hungerbühler et al. , to be published.

⁷ A. L. Kane, Acta Physica Polonica B3, 845 (1972).

⁸ H. J. Lipkin, Phys. Rev. D7, 846 (1973).

FIGURE CAPTIONS

Fig. 1. Plan view of the negative hyperon beam and apparatus used for this experiment.

Fig. 2. $p-\pi^-$ invariant mass distribution, showing peak at the Λ^0 mass and Λ^0 mass resolution.

Fig. 3(a). Mass distribution of $\Lambda^0 \pi^-$ states with decay vertex in the scintillator target; (b) The unshaded histogram is the mass distribution of the above events after requiring at least a 5 mrad angle between the incident hyperon momentum and the $\Lambda^0 \pi^-$ momentum. The shaded histogram shows the same distribution after the subtraction of background Ξ^- peak determined from decays downstream of the scintillator target.

Fig. 4(a). Deck-effect diagram for $\Sigma^- p \rightarrow \Lambda^0 \pi^- p$. (b) Monte Carlo prediction of $\Lambda^0 \pi^-$ invariant mass distribution due to Deck effect. Note the similarity to the observed spectrum shown as the shaded histogram in Fig. 3(b).

Fig. 5(a). Acceptance of the apparatus as a function of resonance mass for $\Lambda^0 \pi^-$ final states produced within the target. The three curves illustrate different assumed production cross sections, $d\sigma/dt \propto e^{at}$, where $a = 4$ for nondiffractive Σ^{*-} production, $a = 20$ for diffractive excitation on protons, and $a = 60$ for diffractive excitation on ^{12}C . (b) Upper limit (90% confidence level) on the cross section for the production of Σ^{*-} which decay into $\Lambda^0 \pi^-$, assuming $d\sigma/dt \propto e^{4t}$ and a resonance width of 10 MeV.

Fig. 6(a). Acceptance of the apparatus as a function of Ξ^{*-} resonance mass for $\Lambda^0 K^-$ final states produced within the target. Two assumed production cross sections of the form $d\sigma/dt \propto e^{at}$ are shown. (b) Upper limits (90% confidence level) on the cross section for the production of Ξ^{*-} which decay into $\Lambda^0 K^-$. The same two production models are considered.

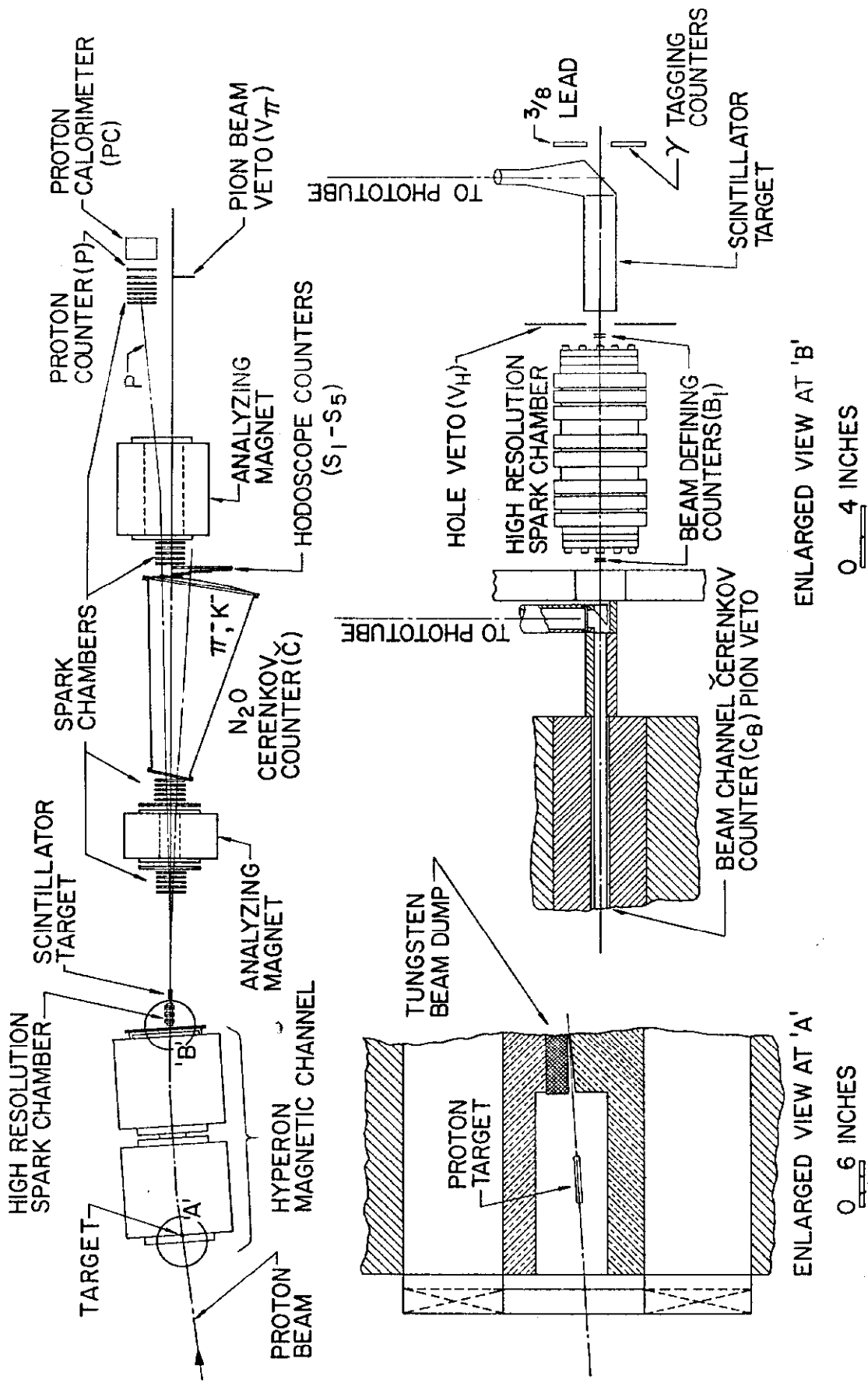


Fig. 1

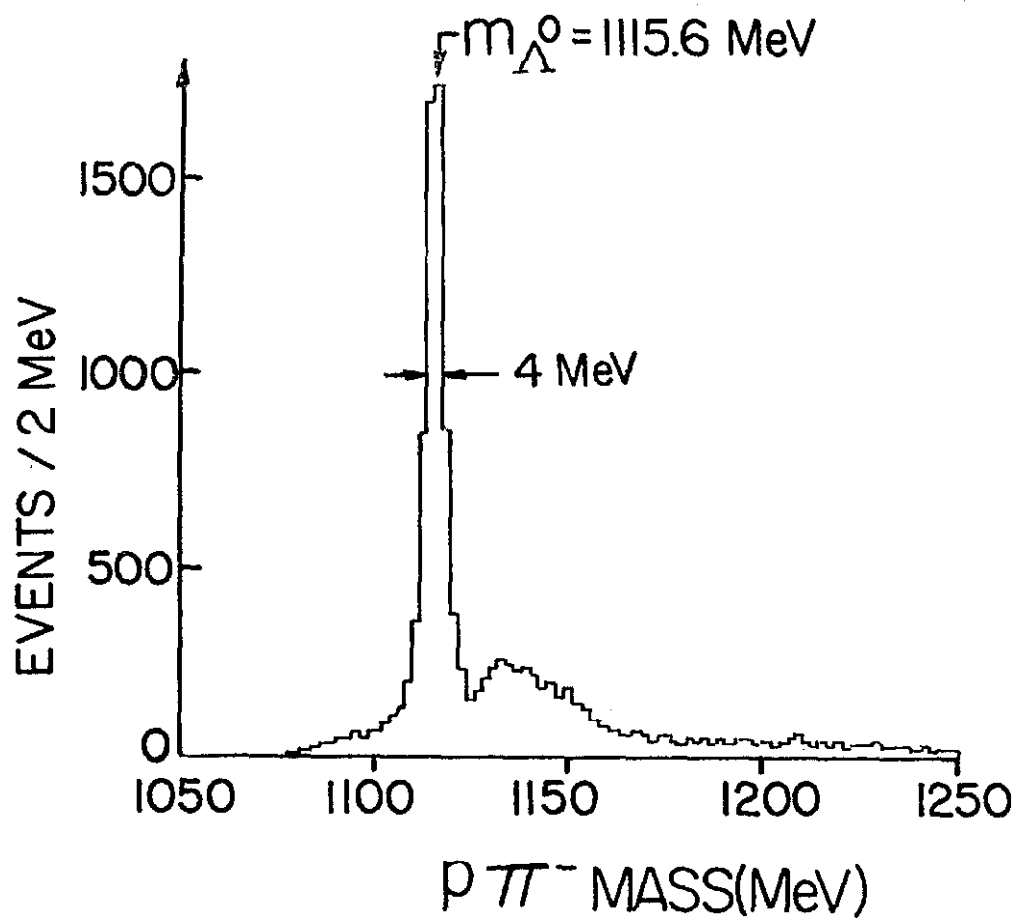


Fig. 2

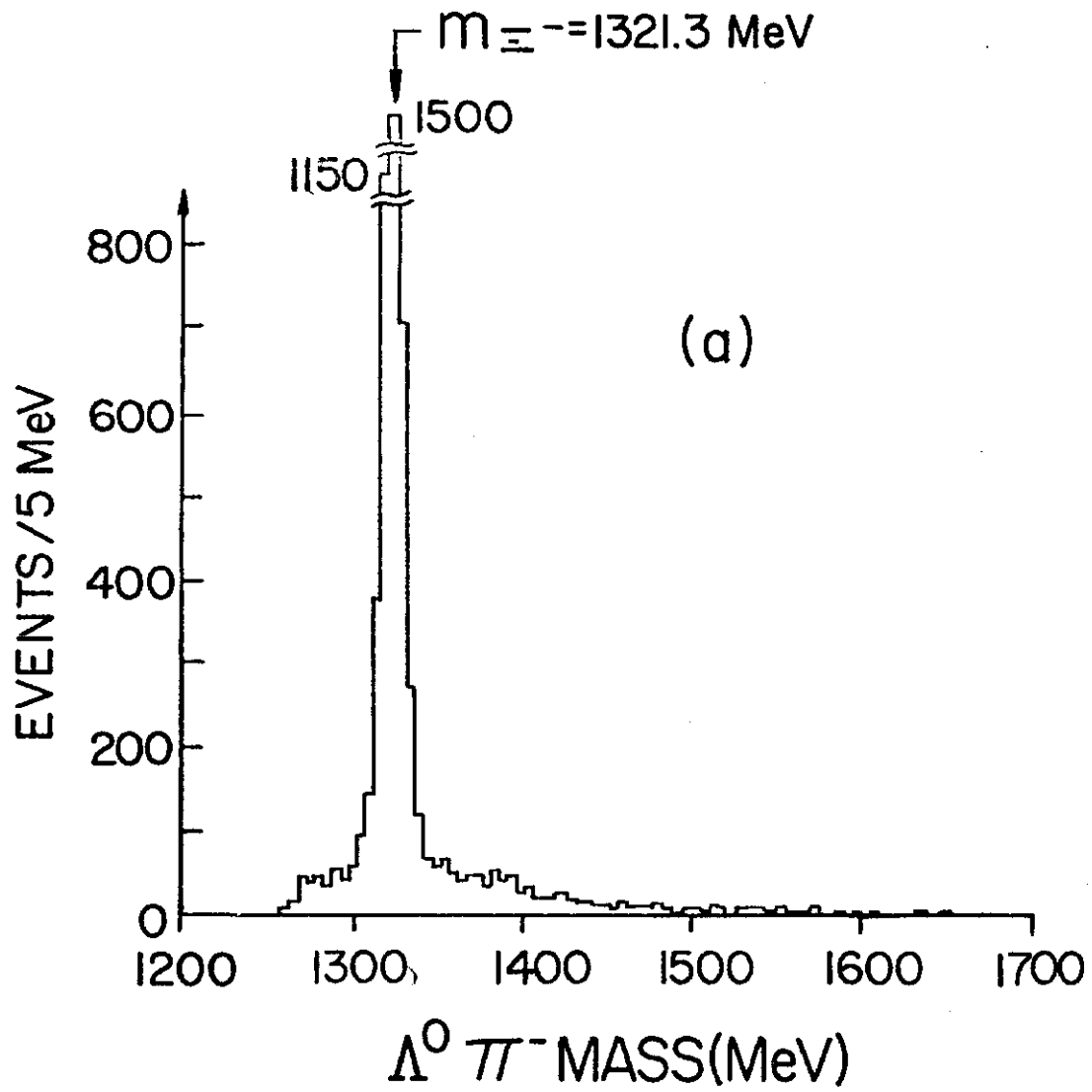


Fig. 3(a)

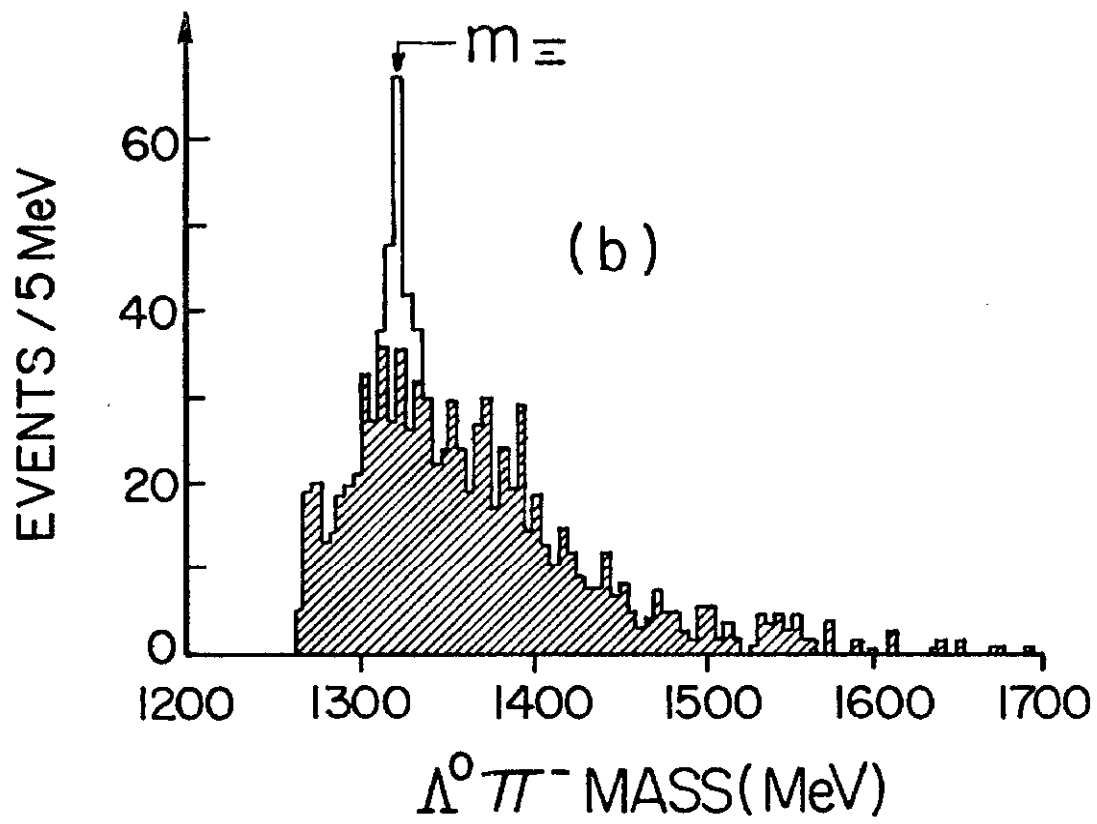


Fig. 3(b)

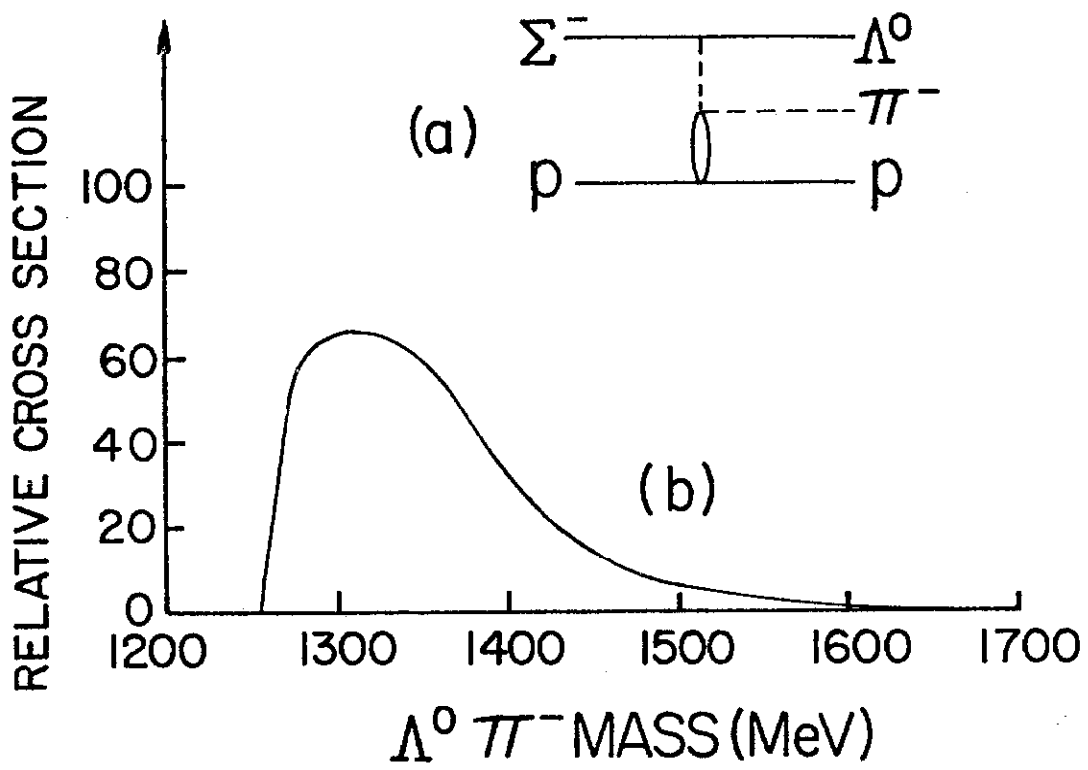


Fig. 4

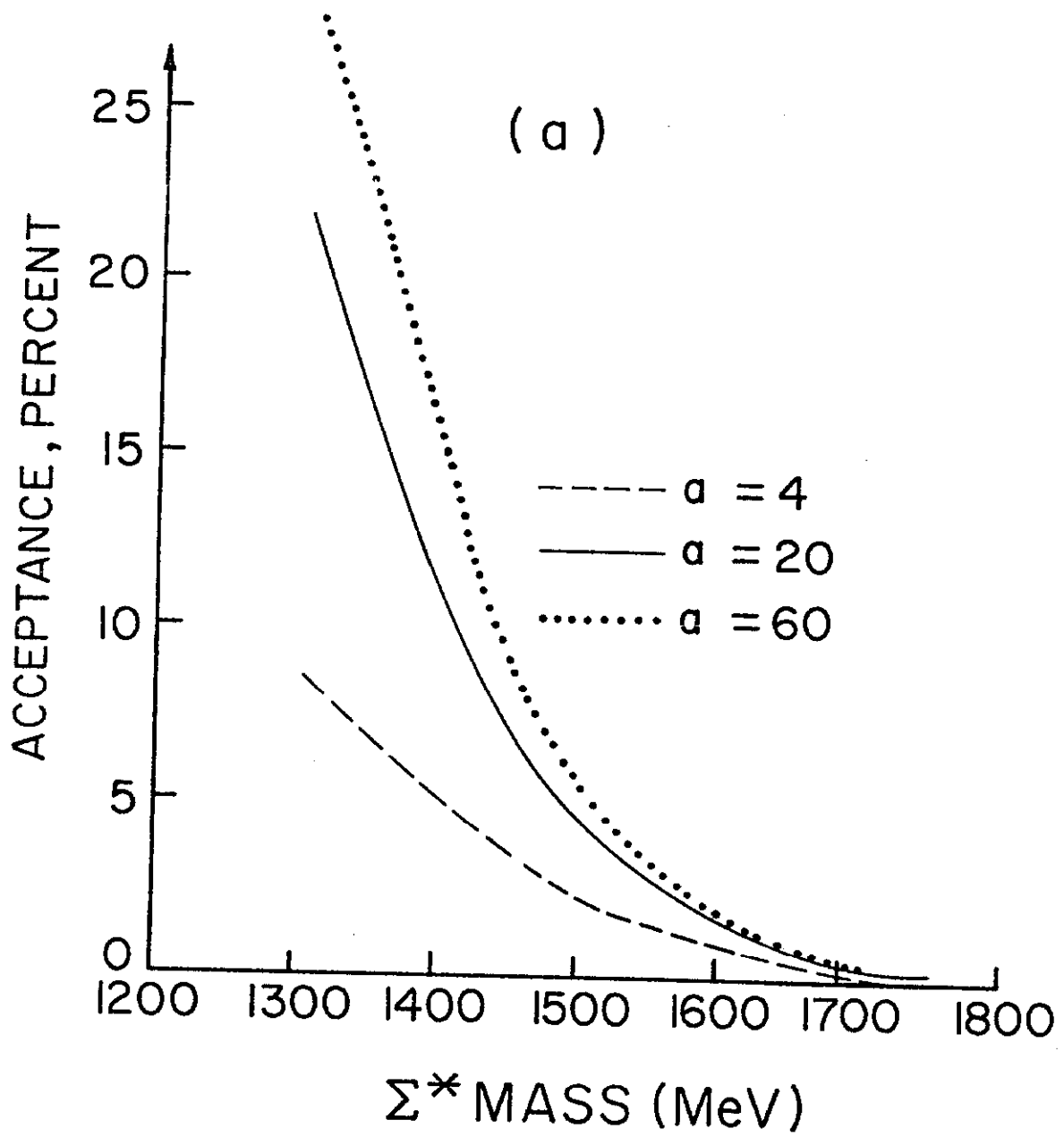


Fig. 5(a)

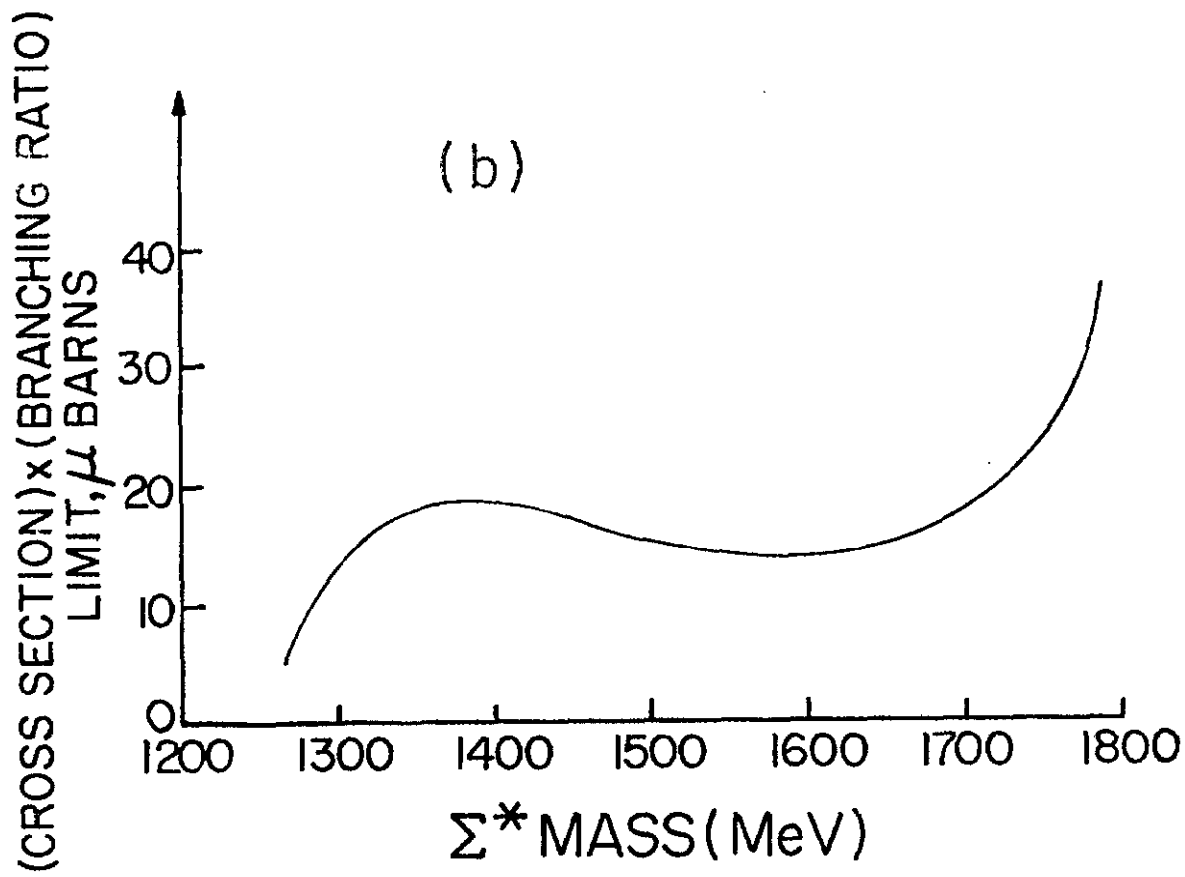


Fig. 5(b)

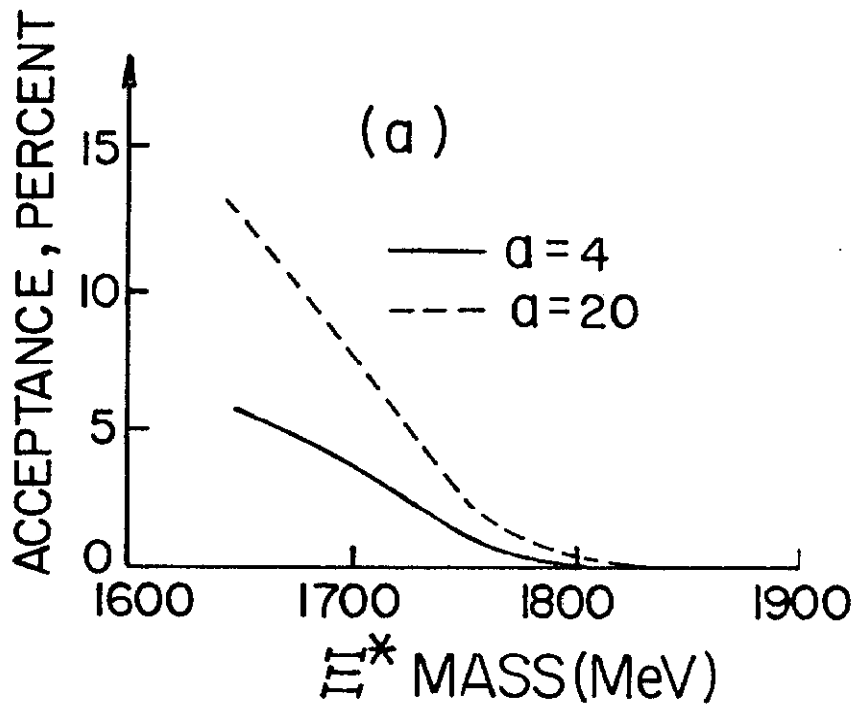


Fig. 6(a)

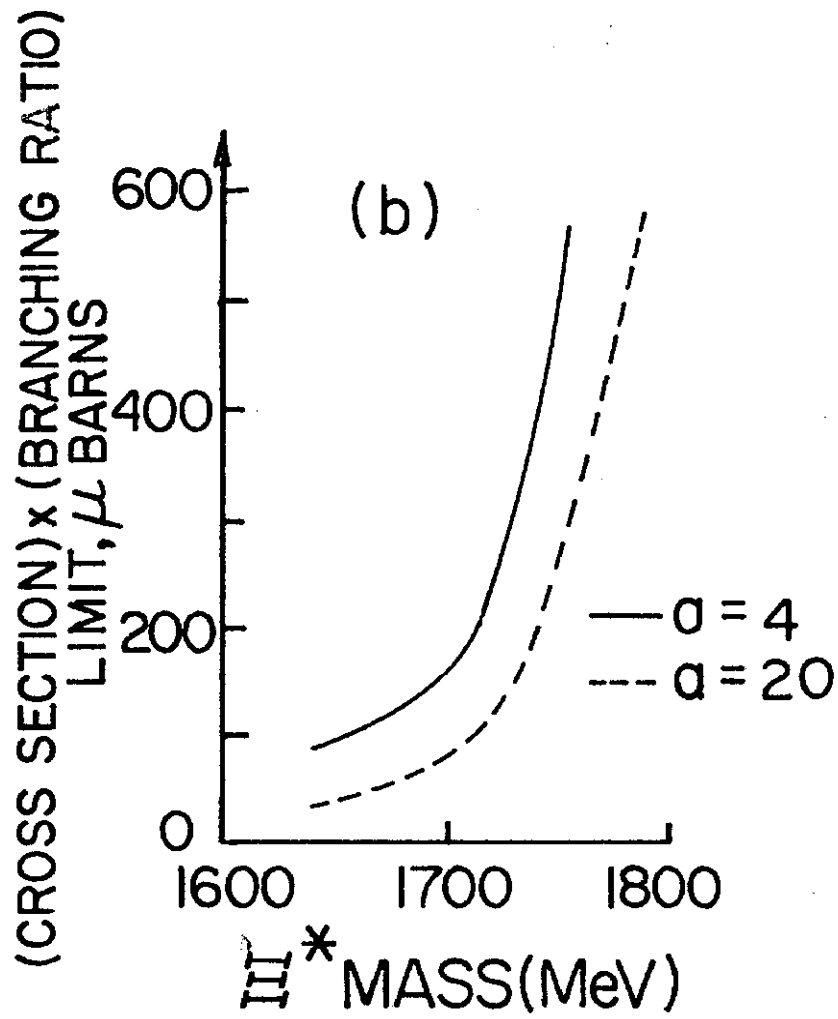


Fig. 6(b)